Dislocation Density Approach to Understanding Sintering Mechanics

Chaoyi Zhu*, Diletta Giuntini^*, Tyler Harrington*, Eugene Olevsky^*, Kenneth Vecchio*

*Department of NanoEngineering and Materials Science and Engineering Program, UC San Diego, La Jolla CA, 92131

^Department of Mechanical Engineering, San Diego State University, CA 92182

UC San Diego

SAN DIEGO STATE UNIVERSITY

Shrinkage Anisotropy in Uniaxial Cold-Pressed Green Compact

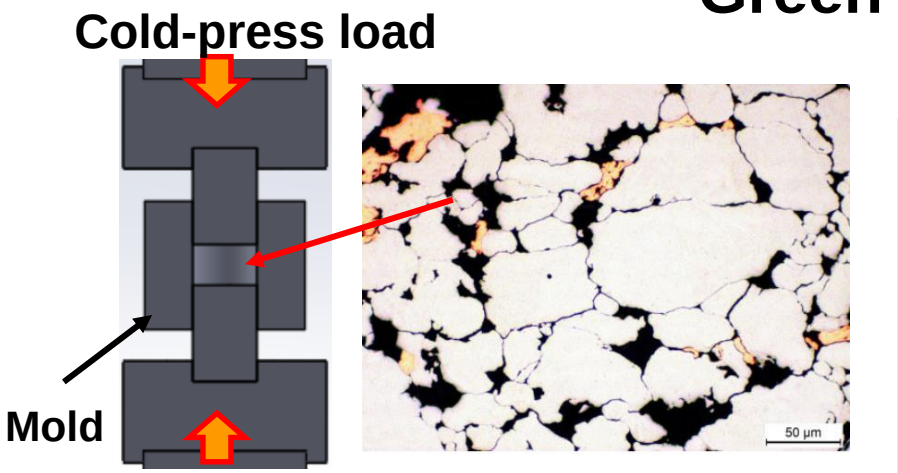

Fe-3Cu-0.5C green compact

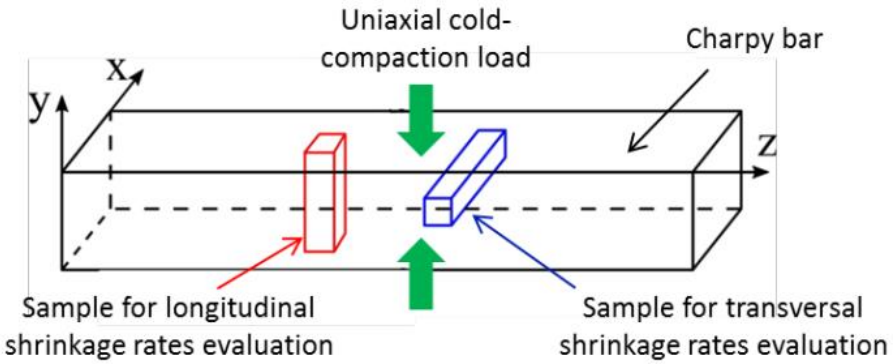

Shrinkage anisotropy arises from inhomogeneity in prior compaction.

- Zavaliangos *et al*.: different 'quality' of grain boundaries in terms of interface pores and oxide fragmentation
- **Molinari *et al.*: volume diffusion through dislocation pipe diffusion dominates over grain boundary diffusion**

Reference:
Molinari *et al*., Powder Metallurgy, 2013
Zavaliangos *et al*., Science of Sintering, 2006

Shrinkage Anisotropy in Uniaxial Cold-Pressed Green Compact

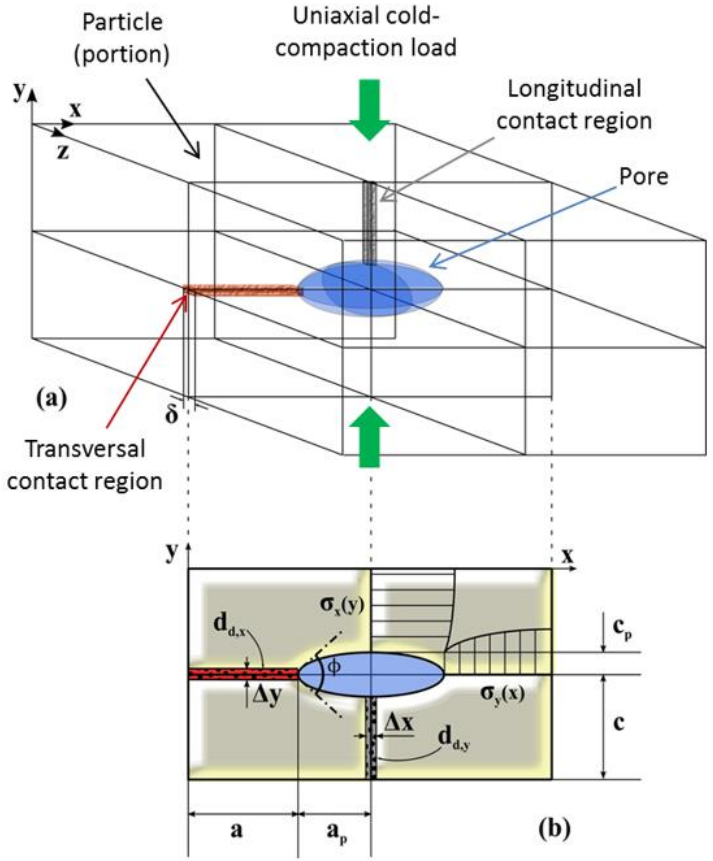

Schematics of the study domain representative of the porous material's structure

- Pressure-less sintering model in longitudinal (y) and transverse (x) directions (Giuntini *et al.*)
- Adapted from Prof. Olevsky's micromechanical model (2005) for grain boundary and surface diffusion
- Enhanced volume diffusion through dislocation pipe diffusion under severe plastic deformation

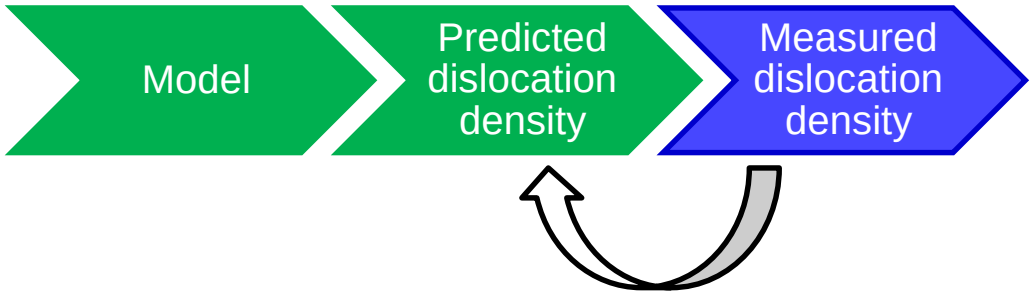

Reference:
Olevsky *et al*., Philosophical Magazine, 2005

Nanoindentation

Indentation Size Effect (Pharr *et al*.)

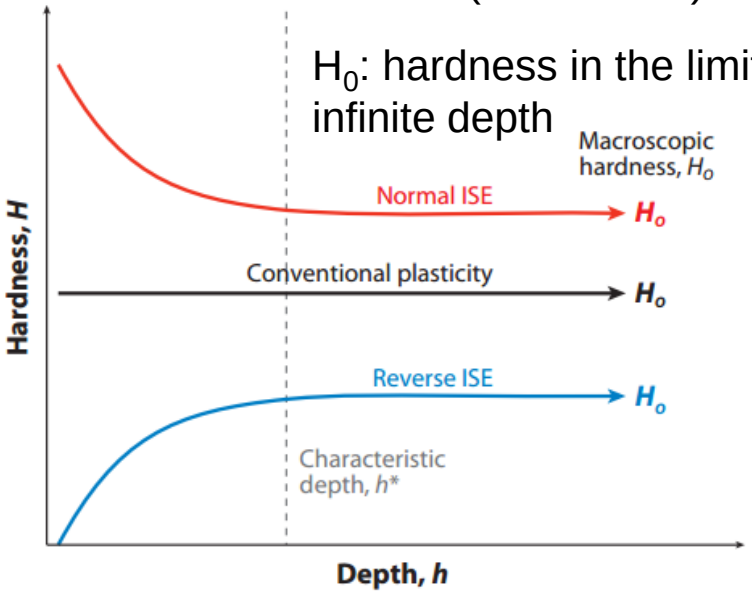

Hardness (H) vs contact depth (h) plot (Pharr *et al.)*

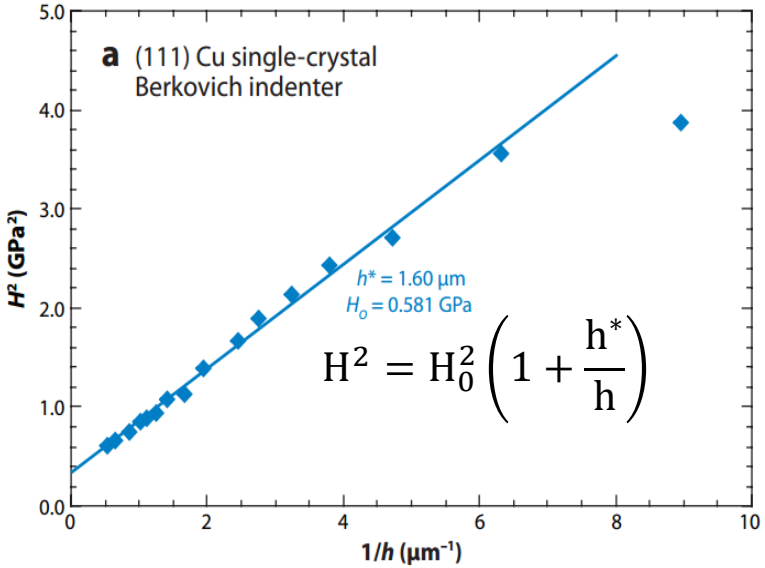

Nix and Gao's (1997) model for determining the pre-existing dislocation density (Θ=65.3° for Berkovich indenter; h*: characteristic depth that depends on the shape of the indenter):

$$\rho = \frac{3\tan^2\theta}{2bh^*}$$

Reference:
Nix and Gao, *Journal of the Mechanics and Physics of Solids*, *1998*
Pharr *et al*., Annual Review of Materials Research, 2010
Oliver and Pharr, Journal of Materials Research, 1992

Nanoindentation Experiment

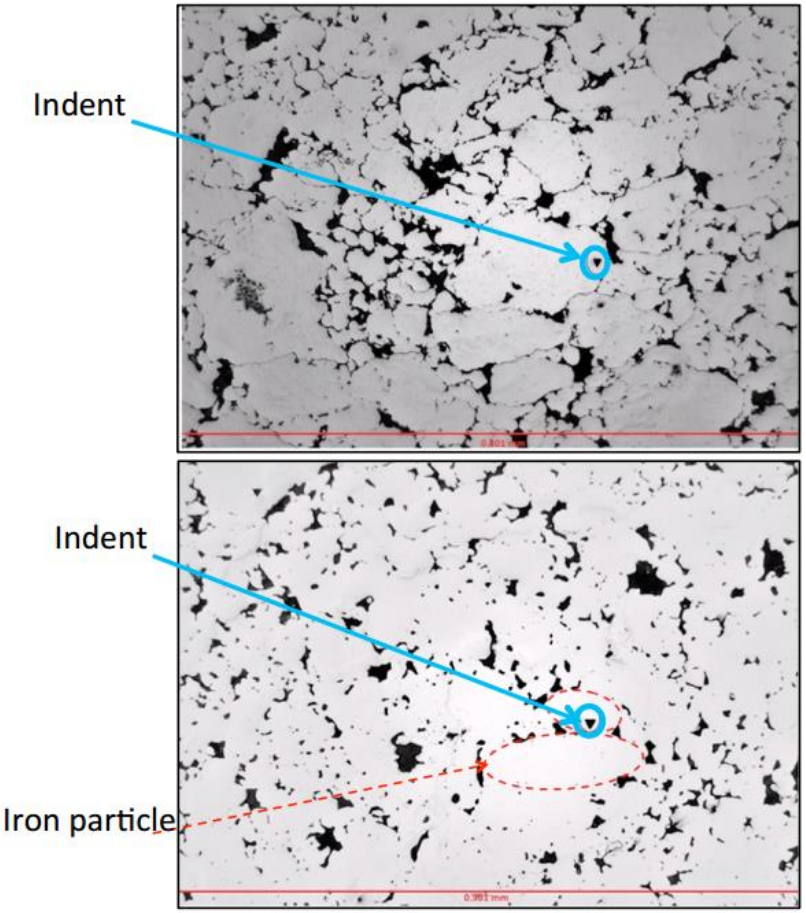

Micrographs of the nanoindentation along a longitudinal and transverse contacts (adapted from Giuntini *et al.*)

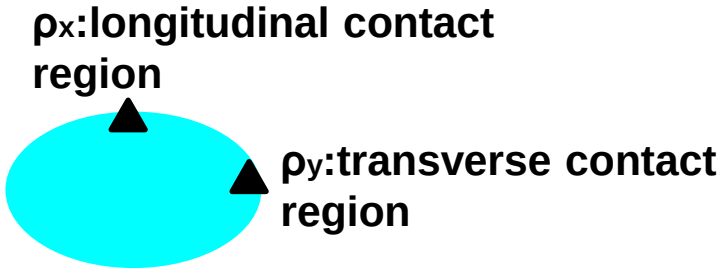

Final polish: 0.05μm colloidal silica + 0.04μm alumina

Indentation forces of 55 mN, 75 mN and 95 mN, with a 20-s holding before unloading.

Samples sintered at 640℃, 730℃, 860℃ and 960℃ were used.

The measurements were carried out in the longitudinal and transverse contacts and then averaged.

Nanoindentation Experiment

Table of total dislocation density values

Temperature (°C)		h^*(m)	ρ ($1/m^2$)
640	y	2.63E-07	4.86E+15
	x	1.92E-07	6.65E+15
730	y	2.21E-07	5.76E+15
	x	1.91E-07	6.69E+15
860	y	7.36E-07	1.74E+15
	x	4.27E-07	2.99E+15
960	y	4.74E-06	2.70E+14
	x	1.36E-06	9.38E+14

$$H^2 = H_0^2\left(1 + \frac{h^*}{h}\right)$$

$$\rho = \frac{3tan^2\theta}{2bh^*}$$

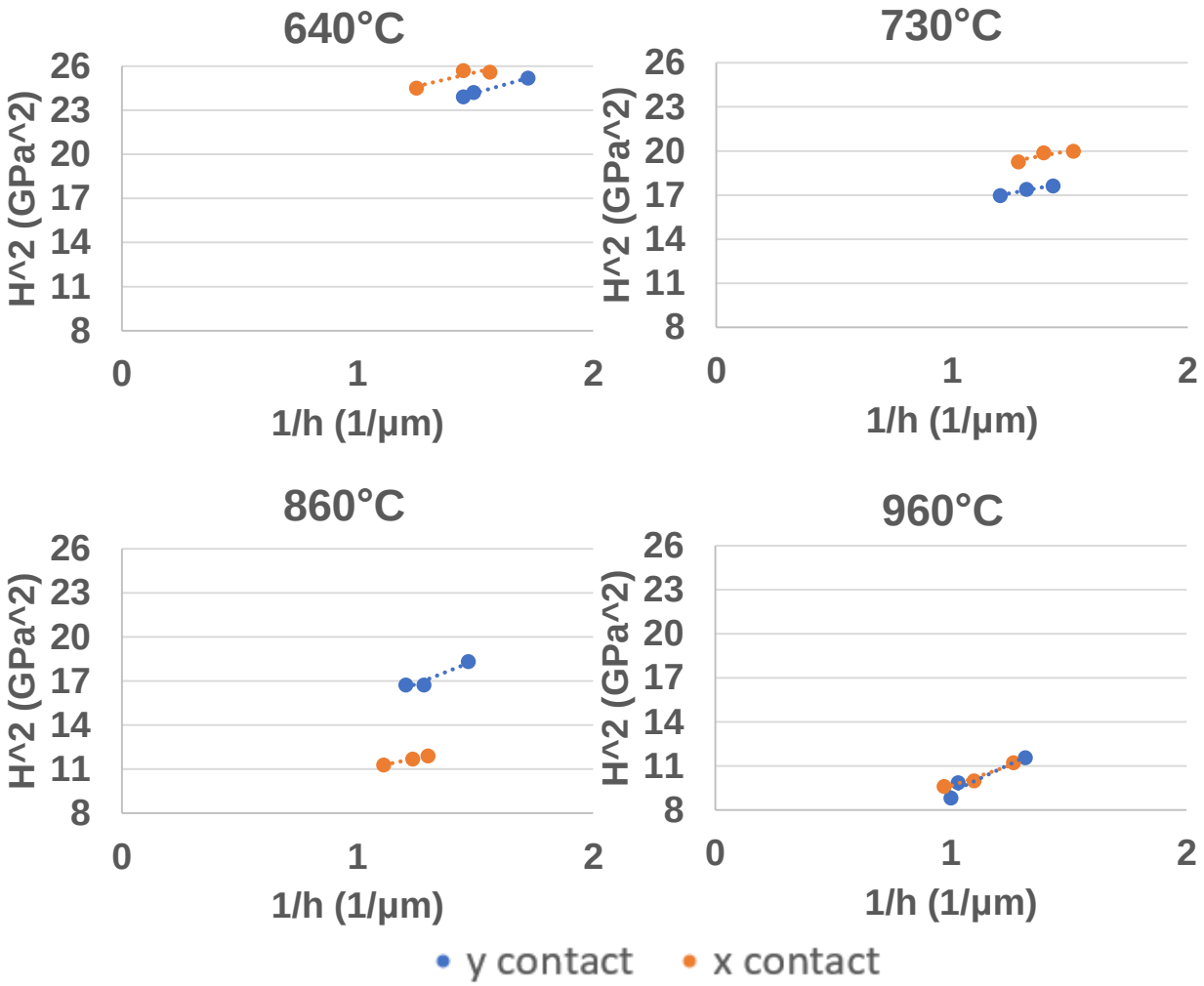

- Higher the sintering temperature, lower the residual dislocation density.
- Dislocation density is higher in longitudinal contacts.

Overview of EBSD-based GND density calculation

Schematic of Geometrically-necessary (GND) and Statistically-stored (SSD) dislocations

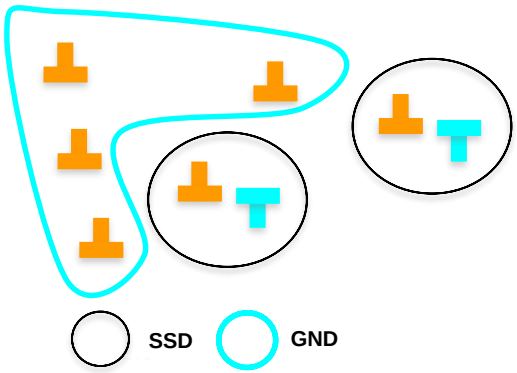

GND in a crystal (e.g. bending)

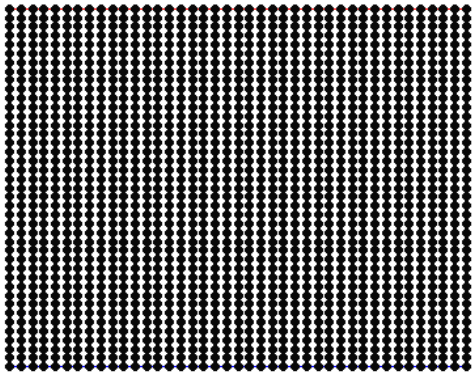

- Accommodate lattice curvature associated with non-uniform deformation

Nye's dislocation density tensor relates lattice orientation gradients to dislocation density (Nye 1953)

$$\alpha_{ij} = \sum_{n=1}^{N} \rho_{GND}^{n} b_i^n l_j^n$$

$$\alpha = \begin{bmatrix} \frac{\partial \omega_{12}}{\partial x_3} - \frac{\partial \omega_{13}}{\partial x_2} & \frac{\partial \omega_{13}}{\partial x_1} & \frac{\partial \omega_{21}}{\partial x_1} \\ \frac{\partial \omega_{32}}{\partial x_2} & \frac{\partial \omega_{23}}{\partial x_1} - \frac{\partial \omega_{21}}{\partial x_3} & \frac{\partial \omega_{21}}{\partial x_2} \\ \frac{\partial \omega_{32}}{\partial x_3} & \frac{\partial \omega_{13}}{\partial x_3} & \frac{\partial \omega_{31}}{\partial x_2} - \frac{\partial \omega_{32}}{\partial x_1} \end{bmatrix}$$

Extract the lattice orientation gradients (Demir *et al*. 2009)

$$\alpha_{ik} = -\epsilon_{klj} \frac{\partial \beta_{ij}^{el}}{\partial x_l} \approx -\epsilon_{klj} g_{ij,l}$$

Solve for dislocation density vector ρ using Matlab under the the L1 dislocation energy minimization scheme (Britton *et al.* 2012)

$$\boldsymbol{\alpha} = \boldsymbol{\xi}(6\times33) \cdot \boldsymbol{\rho}(33\times1) = \boldsymbol{\Lambda}(6\times1) \qquad \text{HCP(N=33)}$$

GND resolution is limited by angular resolution and step size (Wilkinson and Randman, 2010)

Reference:
Zhu *et al*., Acta Materialia, 2016
Nye, Acta Metallurgica,1953
Demir *et al*., Acta Materialia, 2009
Britton *et al.,* Acta Materialia, 2012
Wilkinson *et al.,* Philosophical Magazine, 2010

EBSD based GND calculation

Step 1: Find Particle Boundary

Step 2: EBSD Scan

Step 3: GND Calculation

Step 4: Boundary Mask

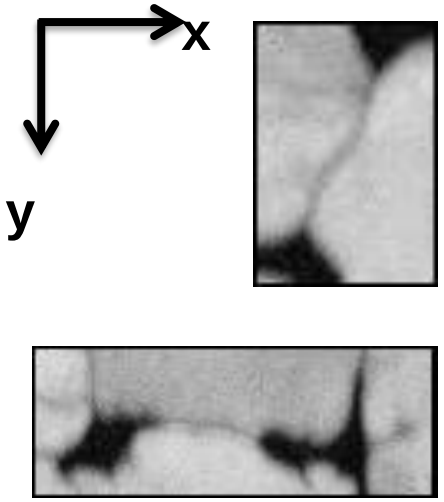

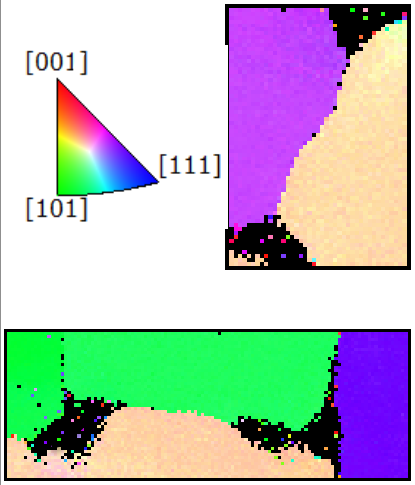

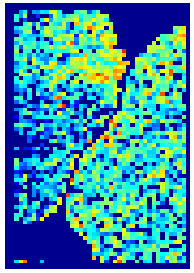

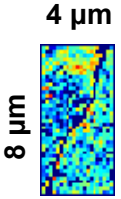

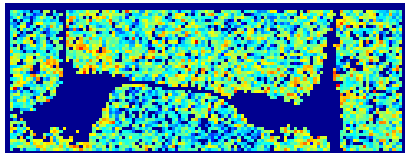

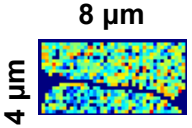

20µm

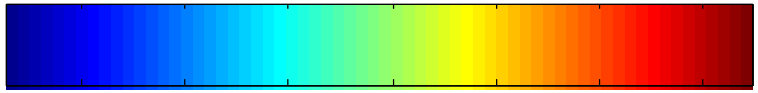

Noise floor: 10^{14} per m^2

EBSD based GND calculation

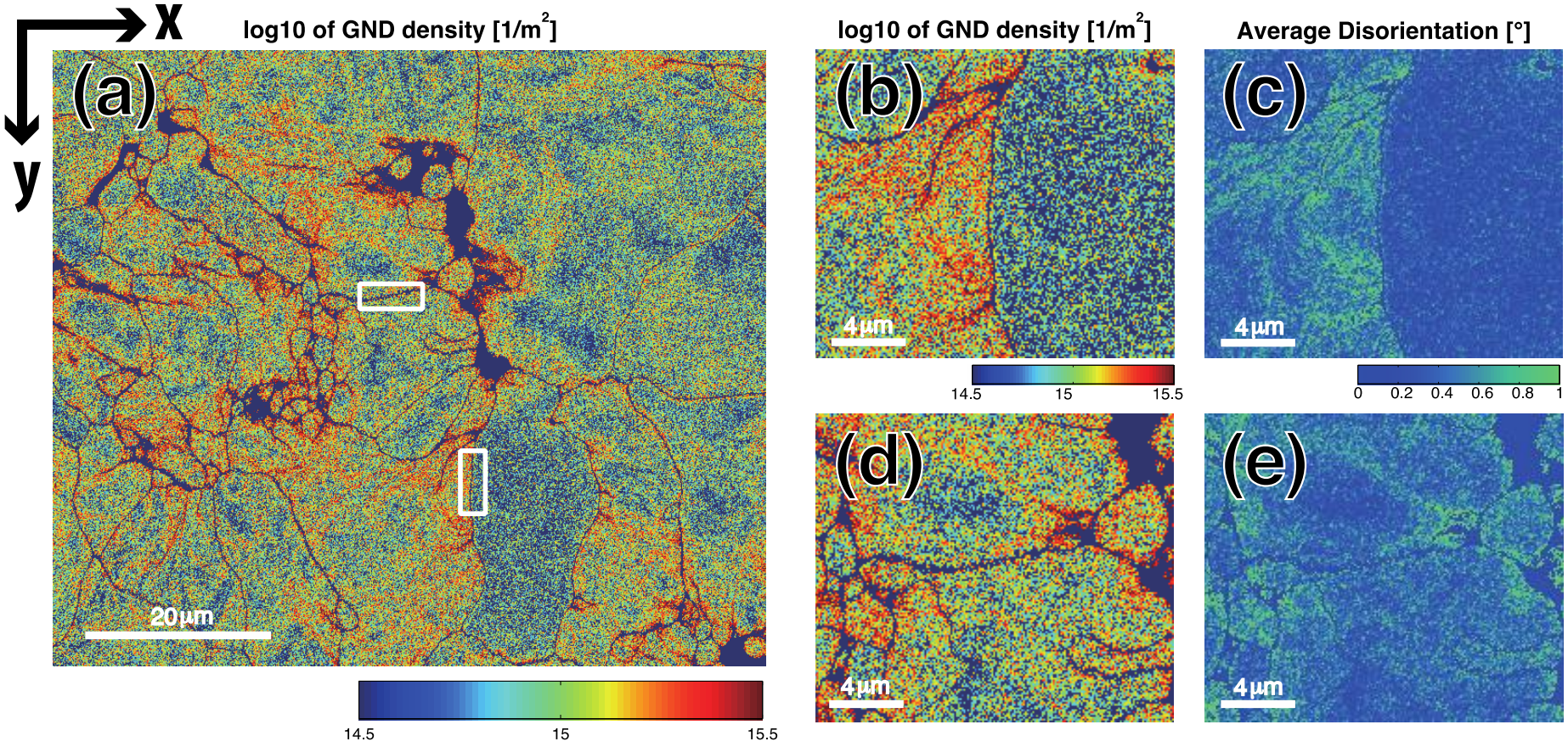

Regions of higher GND density are near the contacts of particles.

Comparison of GND density and total dislocation density

Total dislocation density (nanoindentation)=GND (EBSD)+SSD

GND density

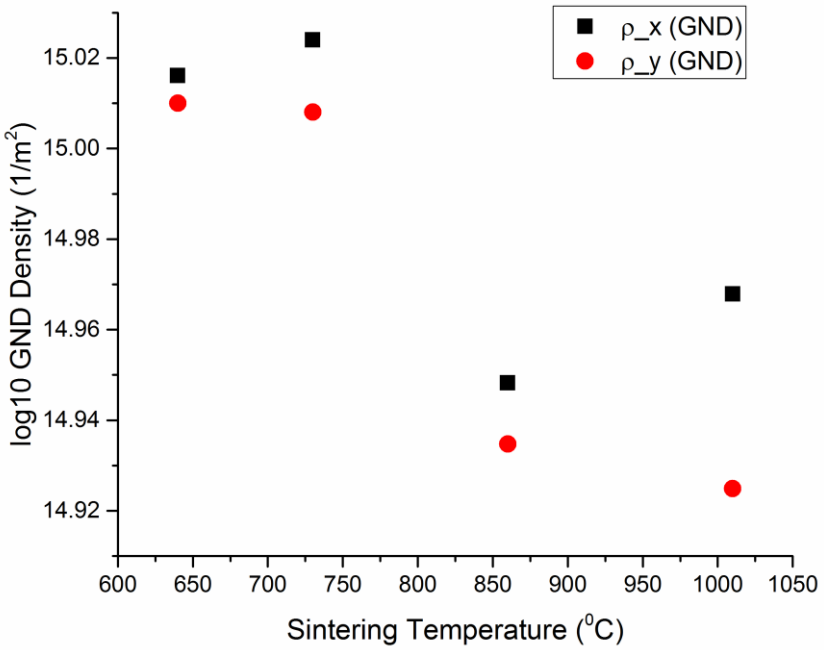

GND density & total dislocation density

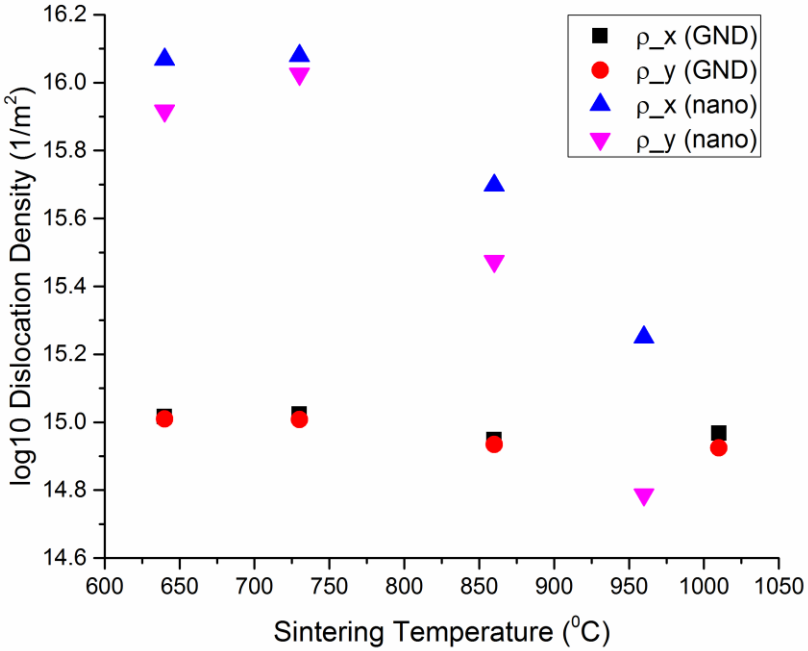

- The difference between total dislocation density and GND density shrinks as thermal annihilation of SSD is enhanced at increasing temperature.
- GNDs are relatively less sensitive to change in sintering temperature.
- Mass transport is mainly through SSDs at low sintering temperature.

Model Validation

Predicted total dislocation density results versus measured dislocation density

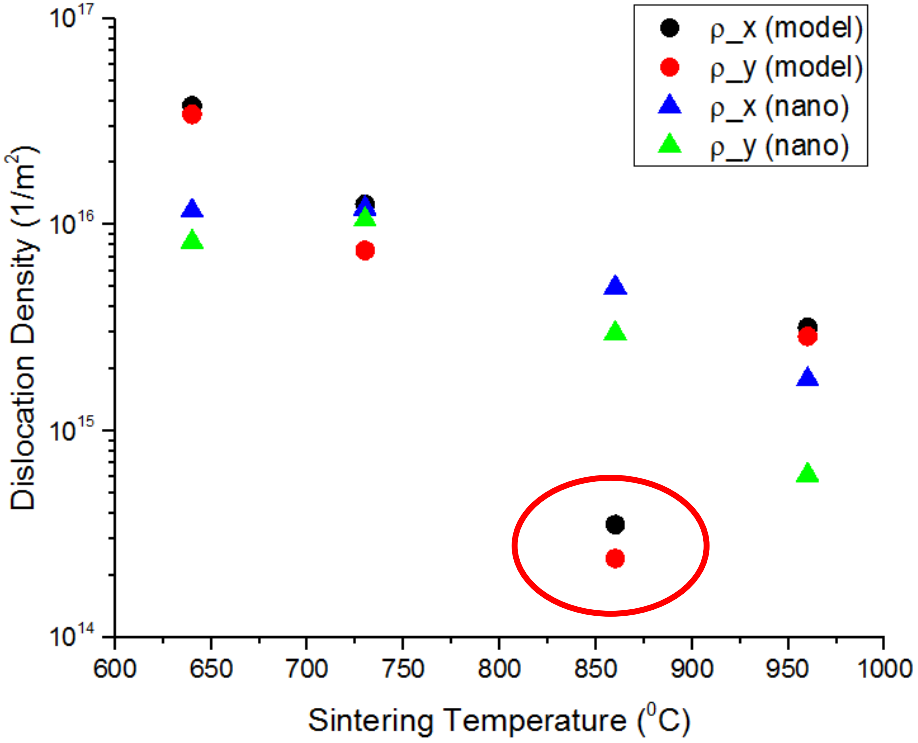

Ratio between modeled and experimentally determined dislocation density

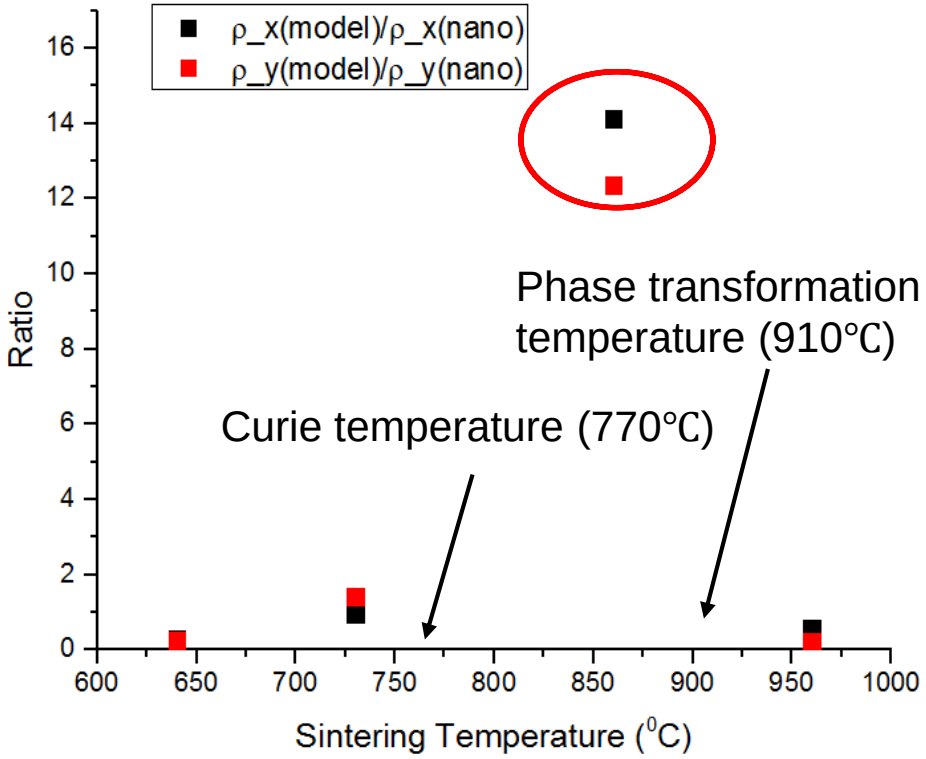

- Model validation reveals disagreement at sintering temperature 860℃
- The measured value at 860℃ is an order of magnitude larger than model prediction. Why?

Diffusivity data

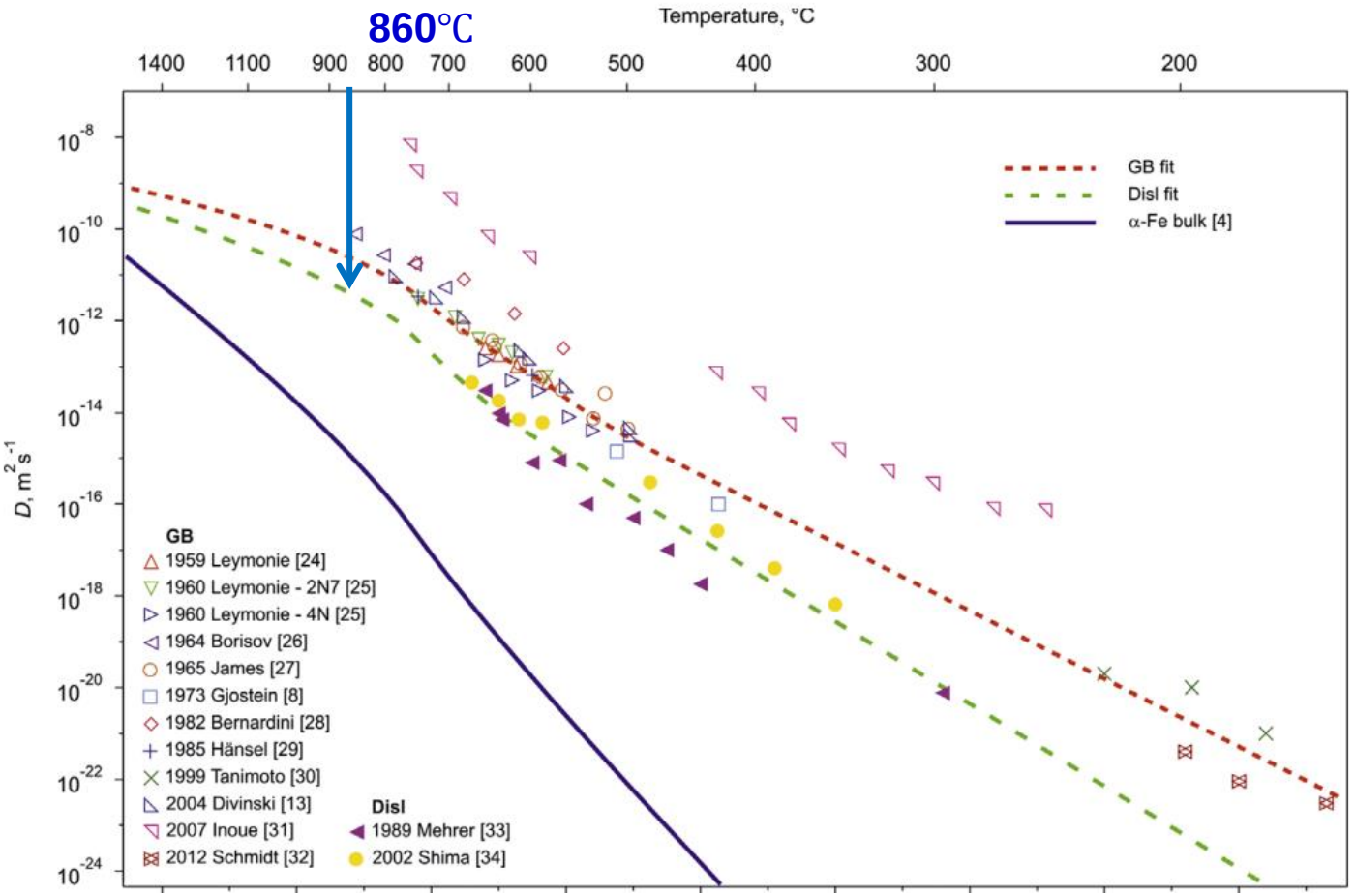

There is a lack of literature values of pipe diffusivity data for ferrite above 770℃

Stechauner and Kozeschnik, 2014; Shima *et al.,* Materials Transactions, 2002

Parametric Study

Predicted total dislocation density results versus measured dislocation density

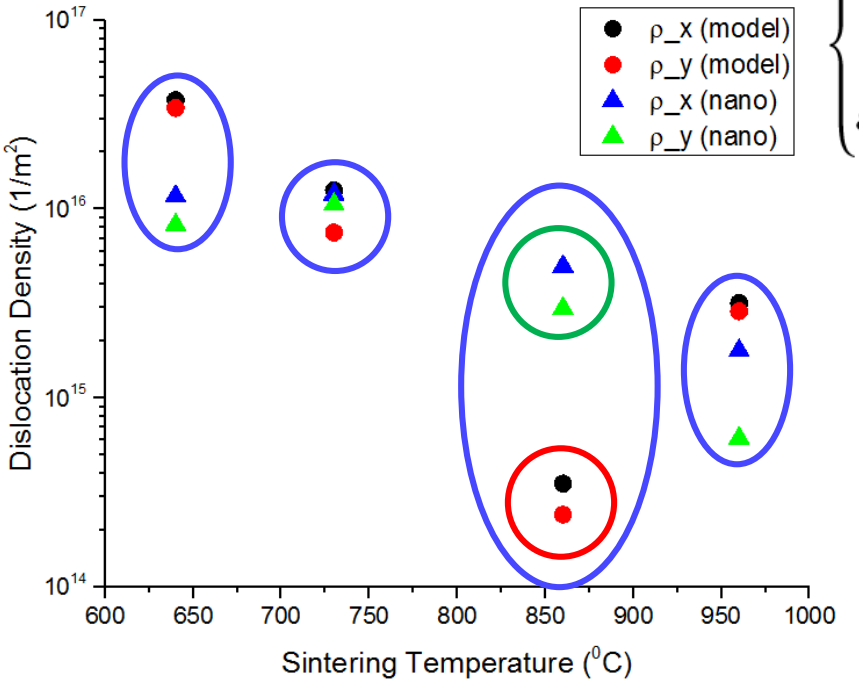

Proposed model:

$$\begin{cases} \dot{\varepsilon}_x^{f.s.} = -3\dfrac{D_V\left(1+\pi\cdot r_p^2\cdot\rho_y\cdot\frac{Dp}{D_V}\right)\cdot\Omega}{k\,T\delta}\gamma_{sv}\dfrac{\mathrm{S_p}/2}{(a+a_p)(c+c_p)c}\left[\dfrac{1}{r_c}-\dfrac{1}{c}\sin\dfrac{\phi}{2}\right] \\ \dot{\varepsilon}_y^{f.s.} = -3\dfrac{D_V\left(1+\pi\cdot r_p^2\cdot\rho_x\cdot\frac{Dp}{D_V}\right)\cdot\Omega}{k\,T\delta}\gamma_{sv}\dfrac{\mathrm{S_p}/2}{(c+c_p)(a+a_p)a}\left[\dfrac{1}{r_a}-\dfrac{1}{a}\sin\dfrac{\phi}{2}\right] \end{cases}$$

Model parameters

① Pore or Particle Geometry
- a and c (particle semi-axis)
- a_p and c_p (pore semi-axis)

② Shrinkage rate
- $\dot{\varepsilon}_x^{f.s}$ and $\dot{\varepsilon}_y^{f.s}$

③ Diffusivity
- **D_p** and D_v

Parametric study shows that literature value of pipe diffusivity is an overestimate.

Shima *et al*., Materials Transactions, 2002

Model Validation with Updated Pipe diffusivity

Table for pipe diffusivity data

	Temperature (℃)	D_p (m^2/s)
α-Fe	640	1.63E-14
	730	1.74E-13
	860	3.20E-13
γ-Fe	960	6.56E-13
	1010	1.33E-12

Predicted total dislocation density results versus measured dislocation density

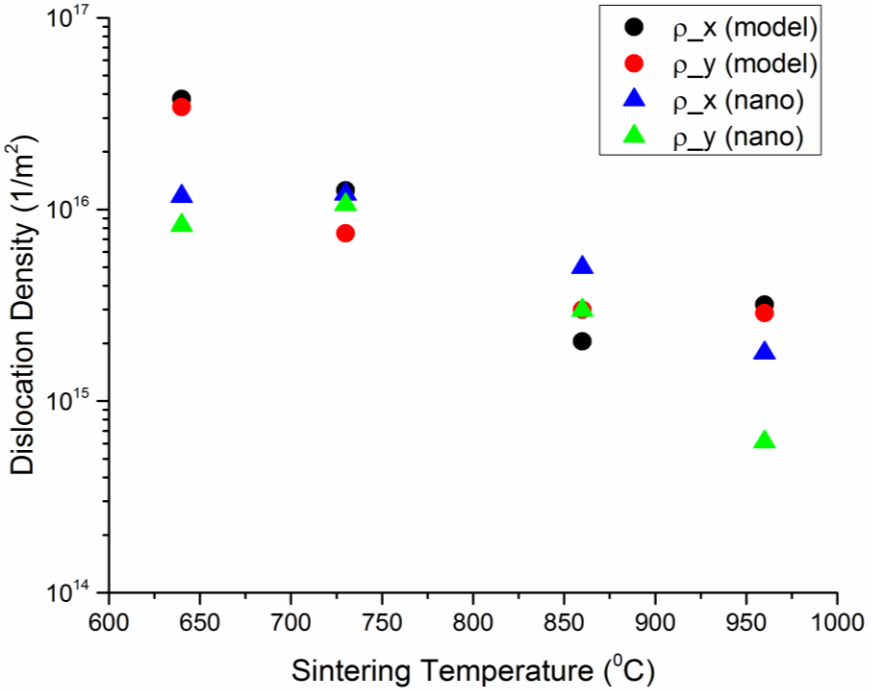

- Overestimate of pipe diffusivity could lead to significant error in model prediction
- The model works well for updated pipe diffusivity value

Summary

- Regions of higher GND density are near the contacts of particles. Total dislocation density and GND density are higher on the longitudinal contacts.
- GNDs are relatively less sensitive to change in sintering temperature. However, SSDs are very responsive.
- Mass transport is mainly through SSDs at low sintering temperatures but through both SSDs and GNDs at very high sintering temperatures.
- The parametric study suggests that the literature value for pipe diffusivity is probably an overestimate.


Thank you!

Backup slides

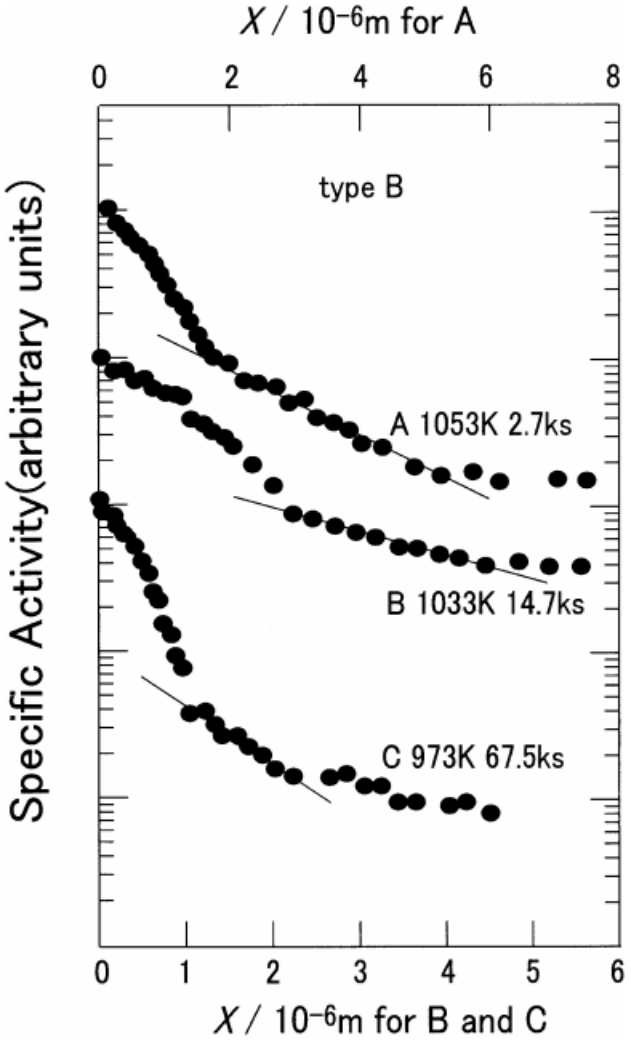

A type: lattice diffusion distance is longer than the dislocation separation

B type: diffusion taking place simultaneously from the surface into the bulk and down and out of dislocations into the surrounding lattice

C type: lateral diffusion zones surrounding the dislocations not influenced by neighboring dislocations

Examples of penetration profiles for self-diffusion along dislocations of in *α*-Fe

Shima *et al*., Materials Transactions, 2002

Pressure-less Sintering in Dilatometer

Green Specimen

- Iron power (d<45 μm) mixed with 0.6 wt% amide wax
- Uniaxial cold compaction
- Green density ~6.9 g/cm^3

Sample

- Debinding at 500 °C for 1 hour
- Samples are cut along the longitudinal and transversal directions

Sintering

- Isothermally sintered for 1 hour at 640 °C, 730 °C, 860 °C, 960 °C and 1010 °C
- Shrinkage and shrinkage rate data are saved

D_V: volume diffusivity

$$\text{Ratio} = \frac{\rho\ (\text{model, arbitrarily reduced } D)}{\rho(\text{model, literature } D_V)}$$

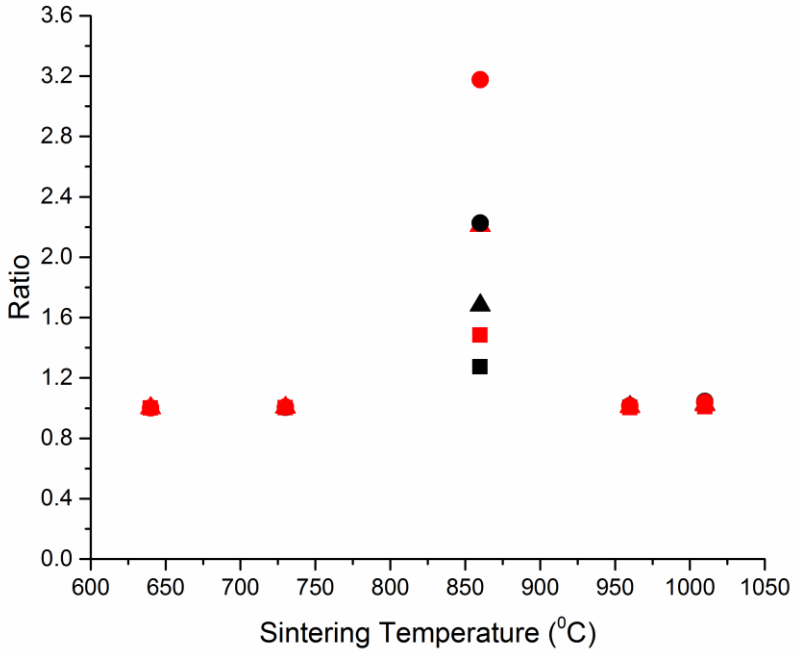

D_p: dislocation pipe diffusivity

$$\text{Ratio} = \frac{\rho\ (\text{model, arbitrarily reduced } D_p)}{\rho(\text{model, literature } D_p)}$$

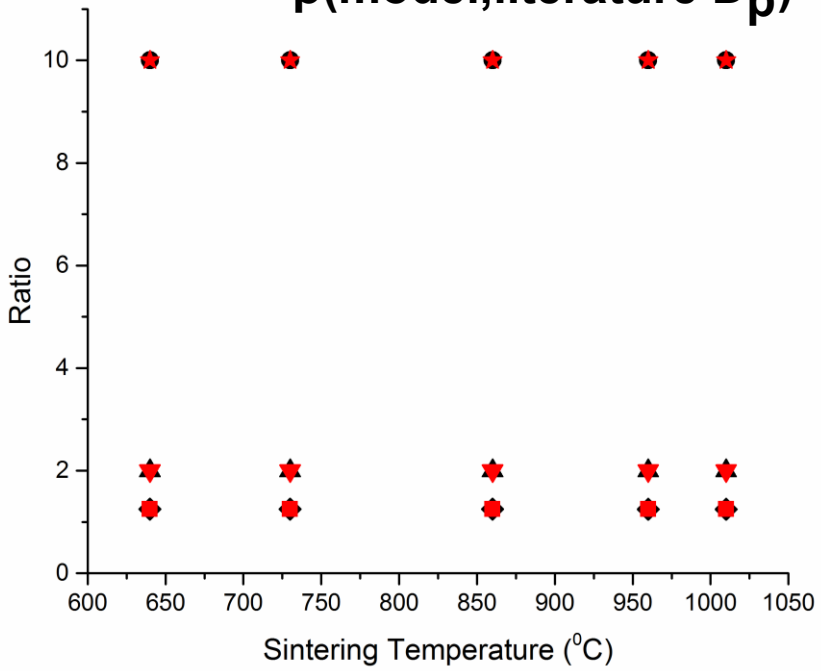

Effect on increasing a or c (particle semi axis)

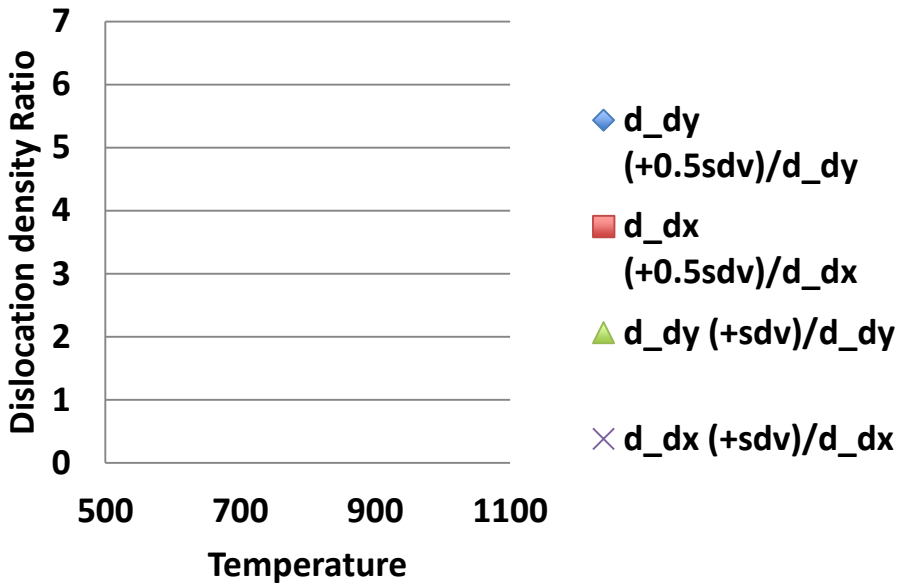

Effect on increasing strain rates

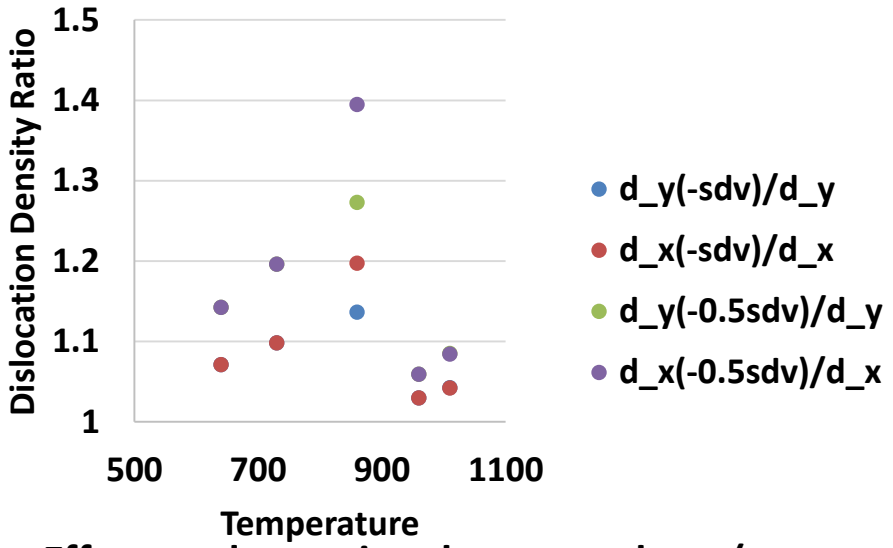

Effect on decreasing the a_p and c_p (pore semi axis)